Region-Specific Alterations in Astroglial TWIK-Related Acid-Sensitive K^+-1 Channel Immunoreactivity in the Rat Hippocampal Complex Following Pilocarpine-Induced Status Epilepticus

JI-EUN KIM,[1,2] SUNG-EUN KWAK,[1,2] SOO-YOUNG CHOI,[2,3] AND TAE-CHEON KANG[1,2]*

[1]Department of Anatomy and Neurobiology, College of Medicine, Hallym University, Chunchon 200-702, South Korea

[2]Institute of Epilepsy Research, College of Medicine, Hallym University, Chunchon 200-702, South Korea

[3]Department of Biomedical Sciences, College of Life Science, Hallym University, Chunchon 200-702, South Korea.

ABSTRACT

In the present study, we performed an analysis of tandem of P domains in a weak inwardly rectifying K^+ channel (TWIK)-related acid-sensitive K^+ (TASK)-1 channel immunoreactivity in the rat hippocampal complex following pilocarpine-induced status epilepticus (SE). In control animals, TASK-1 immunoreactivity was strongly detected in astrocytes in the hippocampal complex. One day after SE, TASK-1 immunoreactivity in astrocytes was markedly reduced only in the molecular layer of the dentate gyrus. One week after SE, loss of astrocytes was observed in the molecular layer of the dentate gyrus. At this time point, TASK-1 immunoreactive cells were detected mainly in the subgranular region. These cells had bipolar, elongated cell bodies with fusiform-shaped nuclei and showed vimentin immunoreactivity. Four weeks after SE (when spontaneous seizure developed), typical reactive astrogliosis was observed in the dentate gyrus and the CA1 region. Almost no astrocytes in the molecular layer showed TASK-1 immunoreactivity, whereas astrocytes in the CA1 region showed strong TASK-1 immunoreactivity. These findings indicate that, after SE, TASK-1 immunoreactivity was differentially altered in astrocytes located in different regions of the hippocampal complex, and these changes were caused by astroglial degeneration/regeneration. Therefore, alteration in TASK-1 immunoreactivity may contribute to acquisition of the properties of the epileptic hippocampal complex. J. Comp. Neurol. 510:463–474, 2008.

Indexing terms: TWIK-related acid-sensitive K^+ (TASK) channels; hippocampal complex; dentate gyrus; epilepsy; astrocytes

Status epilepticus (SE) is a medical emergency with significant mortality (DeLorenzo et al., 1995). SE has been defined as continuous seizure activity, and SE involves severe and prolonged hypoxia, enough to induce a sustained encephalopathy (Rossetti et al., 2007). Therefore, SE causes neuronal cell death (Fujikawa, 1995; Rice and DeLorenzo, 1998), epileptogenesis (Rice and DeLorenzo, 1998), and learning impairment (Stewart and Persinger, 2001). SE also induces astroglial death, which plays a role in the epileptogenic mechanism and in determining the pathophysiological profiles of the epileptic hippocampal complex (Bacci et al., 1999; Kang et al., 2006). Some previous studies have demonstrated that various astroglial molecule expression levels are also altered following SE. For example, loss or down-regulation of glutamine syn-

Grant sponsor: Korea Research Foundation; Grant number: KRF-2005-015-E00003; Grant sponsor: Brain Frontier Program of the Korea Science and Engineering Fund; Grant number: M103KV010020-06K2201-02010.

*Correspondence to: Tae-Cheon Kang, Department of Anatomy and Neurobiology, Institute of Epilepsy Research, College of Medicine, Hallym University, Chunchon 200-702, South Korea. E-mail: tckang@hallym.ac.kr

Received 18 July 2007; Revised 24 November 2007; Accepted 24 April 2008

DOI 10.1002/cne.21767

Published online in Wiley InterScience (www.interscience.wiley.com).

thase (GS), glutamate dehydrogenase (GDH), and γ-aminobutyric acid (GABA) transporter-3 (GAT-3) were pronounced in the hippocampi of epilepsy patients and experimental temporal lobe epilepsy models (Fields and Stevens-Graham, 2002; Eid et al., 2004; van der Hel et al., 2005; Kang et al., 2006). Furthermore, the functional properties (responsiveness to glutamate, characteristics of Ca^{2+} oscillations and K^+ buffering) of astrocytes in the epileptic hippocampal complex are also distinct from those in normal astrocytes (Lee et al., 1995; Gabriel et al., 1998).

K^+ channels are ubiquitously expressed in multicellular and unicellular organisms and are among the most heterogeneous group of ion channels identified in terms of structure and function. K^+ channels are multimeric membrane proteins capable of allowing the passage of K^+ ions across the membrane down their electrochemical potential gradient. Among the subfamily of two P domain K^+ channels, tandem of P domains in a weak inwardly rectifying K^+ channel (TWIK)-related acid-sensitive K^+ (TASK)-1 channels act as outwardly rectifying K^+ channels, which are characterized by four putative transmembrane domains. These channels are thought to underlie the leak or background K^+ conductance. This conductance maintains the passive properties of the cell. They have also been implicated in the regulation of excitability by neurotransmitters (Duprat et al., 1997; Leonoudakis et al., 1998; Reyes et al., 1998; Kim et al., 2000; Niemeyer et al., 2006).

In the present study, we investigated the possibility that SE induces a differential expression of TASK-1 channel in astrocytes at different locations in the hippocampal formation, which plays a role in the functional properties of the epileptic hippocampal complex. Here, we show a spatial/temporal differential expression of astroglial TASK-1 in pilocarpine-induced experimental SE, which extends our understanding of the roles of astrocytes in the properties of the epileptic hippocampal complex.

MATERIALS AND METHODS

Experimental animals

This study utilized the progeny of Sprague-Dawley (SD) rats obtained from the Experimental Animal Center, Hallym University, Chunchon, South Korea. The animals were provided with a commercial diet and water ad libitum under controlled temperature, humidity, and lighting conditions (22°C ± 2°C, 55% ± 5% and a 12:12-hour light/dark cycle with lights). The procedures involving animals and their care were conducted in conformity with the institutional guidelines and were in compliance with international laws and policies (NIH *Guide for the care and use of laboratory animals*; NIH Publication No. 80-23, 1996).

Seizure induction

Male SD rats (9 weeks old, n = 35) were treated with pilocarpine (380 mg/kg, i.p.) at 20 minutes after atropine methylbromide (5 mg/kg, i.p.). Among pilocarpine-treated rats, 32 showed acute behavioral features of SE (including akinesia, facial automatisms, limbic seizures consisting of forelimb clonus with rearing, salivation, masticatory jaw movements, and falling). Diazepam (10 mg/kg, i.p.) was administered 2 hours after onset of status epilepticus (SE) and repeated as needed. The other animals (n = 3) showed only acute seizure behaviors during 10–30 minutes. These nonexperienced SE rats were not used in the present study. After SE, animals were observed for 3–4 hours per day in the vivarium for general behavior and occurrence of spontaneous seizures for 4 weeks. In the acute period (1 day after SE, n = 10), animals seemed somnolent and tended to lie down more than the control animals. In the latent (epileptogenic or silent) period (1 week after SE, n = 11), rats showed normal behavior. The onset of spontaneous seizure occurrence was approximately 3–4 weeks after SE (n = 11). Spontaneous seizures were scored grade 3 or greater on the Racine (1972) Scale (i.e., forelimb clonus ± rearing ± falling). These behavioral results were consistent with our previous studies (Kang et al., 2006; Kwak et al., 2006). Age-matched animals (n = 13) were used as controls.

Tissue processing

At designated times (1 day, 1 week, and 4 weeks after SE), animals were anesthetized (urethane, 1.5 g/kg I.P.) and perfused transcardially with phosphate-buffered saline (PBS) followed by 4% paraformaldehyde in 0.1 M PB (pH 7.4). Control animals were also perfused by the same methods. The brains were removed and postfixed in the same fixative for 4 hours. The brain tissues were cryoprotected by infiltration with 30% sucrose overnight. Thereafter, the tissues were frozen and sectioned with a cryostat at 30 μm, and consecutive hippocampal sections were collected in six-well plates containing PBS. For stereological study, all sections of the entire hippocampus were used in some animals.

Antibody characterization

The TASK-1 antiserum was purchased from Chemicon (Temecula, CA; catalog No. AB5250) and was raised in rabbit against a highly purified peptide corresponding to residues 252–269 of human TASK-1. This epitope is specific for TASK-1 and is highly conserved in rat TASK-1 (17/18 residues identical). This antibody identifies a single ~50-kDa band on Western blots of rat brain tissue lysates (manufacturer's information) and has been reported to identify rat astrocytes (Millar et al., 2000; Rau et al., 2006). For negative control, the rat hippocampal tissues were incubated with 1 μg of the antibody, which was preincubated with 1 μg of purified peptide for 1 hour at room temperature.

The glial fibrillary acidic protein (GFAP) antiserum was also purchased from Chemicon (catalog No. MAB3402), which identifies a single ~51-kDa band on Western blots of brain lysates. This antibody was raised against purified porcine GFAP. This antibody has been reported to identify the astrocytes of various animals (manufacturer's information). For negative control, the rat hippocampal tissues were incubated with only the secondary antibody without GFAP antibody (Yang et al., 2005; manufacturer's information).

The vimentin (Vim) antiserum was purchased from Dako Cytomation (Carpinteria, CA; catalog No. M0725). This antibody was raised against purified vimentin from porcine eye lens, and the specific cross-reactivity with rat vimentin was previously tested by immunohistochemistry (Pecchi et al., 2007). Vim antibody labels a single band of 57 kDa corresponding to vimentin. As demonstrated by immunocytochemistry, the antibody cross-reacts with the vimentin-equivalent protein in man, cow, dog, hamster, horse, rhesus and African green monkeys, rabbit, rat, and

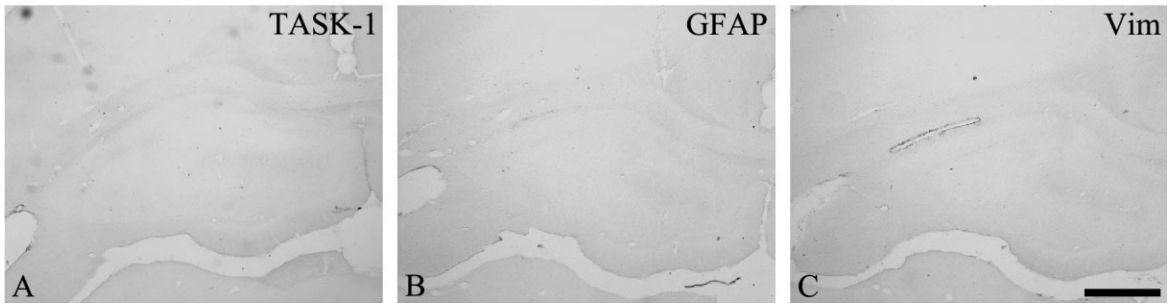

Fig. 1. Results for the hippocampus in the negative control test. The immunohistochemical controls show the absence of any immunoreactivities in all structures. **A:** TASK-1. **B:** GFAP. **C:** Vimentin. Scale bar = 400 μm.

rat kangaroo (manufacturer's information). For negative control, the rat hippocampal tissues were incubated with Dako Cytomation mouse IgG1 (catalog No. X 0931) diluted to the same concentration as the primary antibody (manufacturer's information). All negative controls for immunohistochemistry resulted in the absence of immunoreactivity in any structure (Fig. 1).

Immunohistochemistry and double immunofluorescent staining

The sections were first incubated with 3% bovine serum albumin in PBS for 30 minutes at room temperature. Sections were then incubated in the following primary antibodies in PBS containing 0.3% Triton X-100 overnight at room temperature: mouse anti-GFAP IgG (Chemicon; diluted 1:200) or rabbit anti-TASK-1 IgG (Chemicon; diluted 1:200). The sections were washed three times for 10 minutes each with PBS, incubated sequentially, in biotinylated horse anti-mouse or goat anti-rabbit IgG (Vector, Burlingame, CA) and ABC complex (Vector), diluted 1:200 in the same solution as the primary antiserum. Between incubations, the tissues were washed with PBS three times for 10 minutes each. The sections were visualized with 3,3′-diaminobenzidine (DAB) in 0.1 M Tris buffer and mounted on gelatin-coated slides. The immunoreactions were observed under an Axiophot microscope (Carl Zeiss, Oberkochen, Germany). All images were captured with an Axiocam HRc camera and Axio Vision 3.1 software.

Double immunofluorescent staining for TASK/GFAP was also performed. Brain tissues were incubated in mixture of rabbit anti-TASK-1 IgG (Chemicon; diluted 1:50)/ mouse anti-GFAP IgG (Chemicon; diluted 1:100) overnight at room temperature. After washing three times for 10 minutes with PBS, sections were also incubated in a mixture of FITC- and Cy3-conjugated secondary antisera (Amersham, Arlington Heights, IL; diluted 1:200) for 1 hour at room temperature. Sections were mounted in Vectashield mounting medium with DAPI (Vector). All images were captured using an Axiocam HRc camera and Axio Vision 3.1 software.

Stereology

The hippocampal volumes (V) were estimated according to a formula based on the Cavalieri method: $V = \Sigma P \times a \times t_{nom} \times 1/ssf$, where P is the number of test points falling on the region of the delineated subfield, a is the area of a point grid (100×100 μm^2 in this study), t_{nom} is the nominal section thickness (30 μm in this study), and ssf is the fraction of the sections sampled or section sampling fraction (1 in this study, because we used all sections in the entire hippocampus). The subfield areas were delineated with a ×2.5 objective lens. The volumes are reported as mm^3 (Bedi, 1991; Madeira et al., 1995). The optical fractionator was used to estimate the cell numbers. The optical fractionator (combination of performing counting with the optical disector, with fractionator sampling) is a stereological method based on a properly designed systematic random sampling method that by definition yields unbiased estimates of population number. The sampling procedure is accomplished by focusing through the depth of the tissue (the optical disector height, h; 15 μm in all cases for this study). The number of each cell type (C) in each of the subregions is estimated as: $C = \Sigma Q^- \times t/h \times 1/asf \times 1/ssf$, where Q^- is the number of cells actually counted in the disectors that fell within the sectional profiles of the subregion seen on the sampled sections, and asf is the areal sampling fraction calculated by the area of the counting frame of the dissector, a(frame) (50×50 μm_2 in this study) and the area associated with each x,y movement, grid (x,y step; 250×250 μm_2 in this study) asf = [a(frame)/a(x,y step)]. GFAP and TASK-1 immunoreactivity of the cytoplasm was the criterion followed to identify each cells. The immunoreactive cells were counted with a ×40 objective lens. All immunoreactive cells were counted regardless the intensity of labeling. In addition, analysis of the ratio of TASK-1^+ asctrocytes in $GFAP^+$ astrocytes was performed. Cell counts were performed by two different investigators who were blind to the classification of tissues. SE-induced hippocampal atrophy is evident (Roch et al., 2002; Niessen et al., 2005), so changes in cell number may be caused by an alterations in volume of the hippocampus. Therefore, the total number of cells was corrected by multiplying with appropriate correction factors (CF) representing the degree of shrinkage (or swelling) compared with the control (Shetty and Turner, 2000).

Data analysis

All data obtained from the quantitative measurements were analyzed by using a one-way ANOVA to determine statistical significance. Bonferroni's test was used for post hoc comparisons. A *P* value below either 0.01 or 0.05 was considered statistically significant.

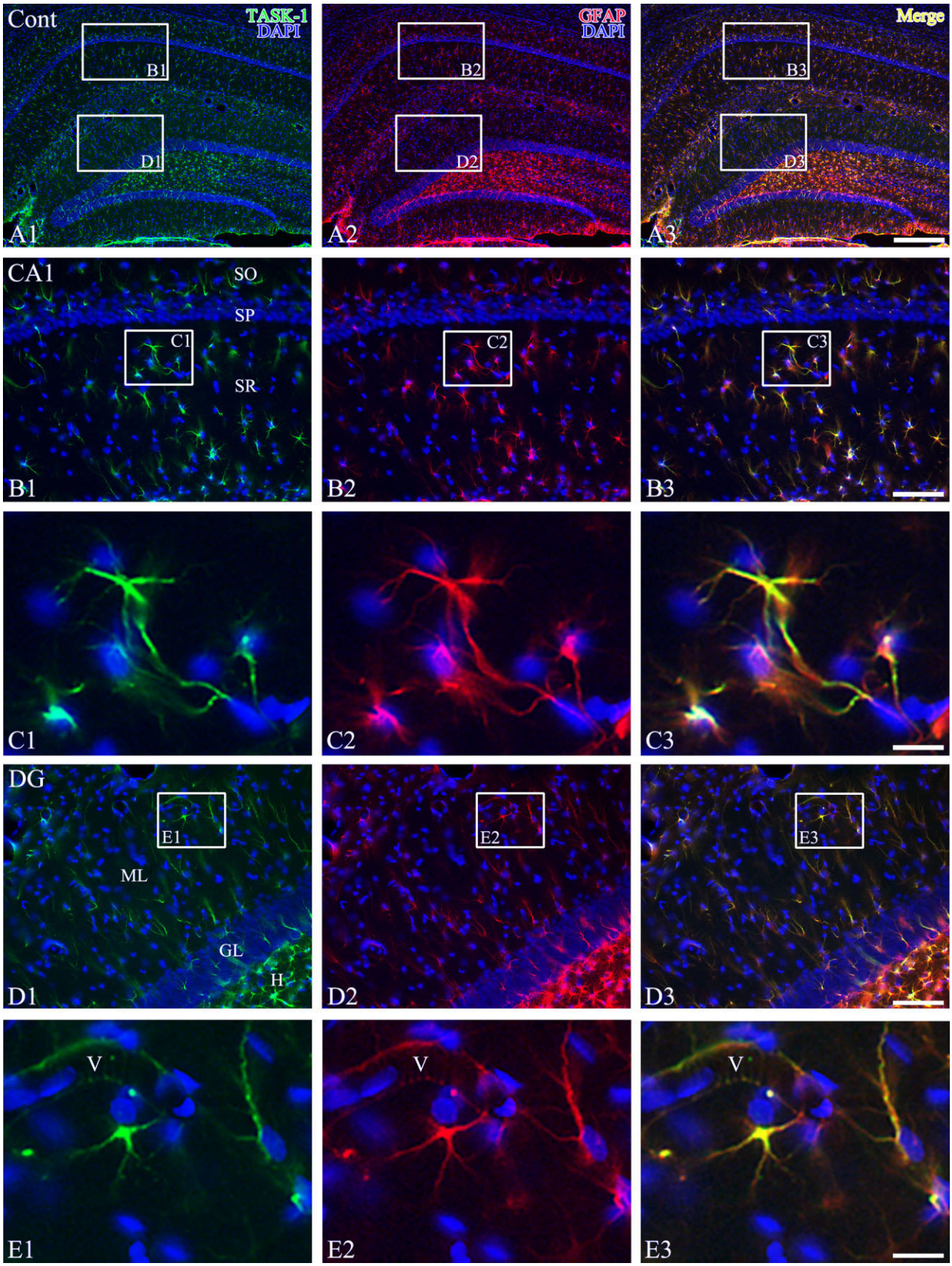

Fig. 2. **A–E:** The localization of TASK-1 (green) and GFAP (red) signals in the control hippocampal complex. TASK-1 immunoreactivity is contained within almost GFAP^{+} astrocytes in the hippocampal complex. Panels 1, 2, and 3 are TASK-1, GFAP, and merged images, respectively. Blue is DAPI counterstaining. GL, granule cell layer; H, hilus; ML, molecular layer; SO, stratum oriens; SP, stratum pyramidale; SR, stratum radiatum; V, vessel. Scale bars = 200 μm in A; 50 μm in B,D; 10 μm in C,E.

TABLE 1. Counting Results From the Stereology of the CA1 Region[1]

				C		CE (C)	
		V (mm^3)	CF	GFAP	TASK-1	GFAP	TASK-1
Control	Mean	11.13	1	248,468	216,846	0.042	0.041
(n = 5)	SEM	0.89	17,393	19,516			
	CV	0.08	0.07	0.09			
1 Day	Mean	11.84	0.94	266,468	226,468	0.039	0.040
(n = 5)	SEM	1.36	23,982	24,911			
	CV	0.12	0.09	0.11			
1 Week	Mean	9.97	1.11	226,489	213,346	0.038	0.037
(n = 5)	SEM	1.21	24,913	17,068			
	CV	0.12	0.11	0.08			
4 Weeks	Mean	8.49[2]	1.31	213,234	198,681	0.048	0.046
(n = 5)	SEM	1.00	27,720	23,842			
	CV	0.12	0.13	0.12			

[1]SEM, standard error of the mean; CV, coefficient of variation; V, volume; CF, correction (shrinkage) factor; C, total number of cells; CE (C), coefficient of error of the total number of cells.
[2]Significant differences from the controls, $P < 0.05$.

TABLE 2. Counting Results From the Stereology of the Molecular Layer of the Dentate Gyrus[1]

				C		CE (C)	
		V (mm^3)	CF	GFAP	TASK-1	GFAP	TASK-1
Control	Mean	7.02	1	86,569	81,329	0.042	0.038
(n = 5)	SEM	0.63	7,791	8,376			
	CV	0.09	0.09	0.10			
1 Day	Mean	7.26	0.97	88,537	62,651[2]	0.041	0.039
(n = 5)	SEM	0.80	9,739	6,516			
	CV	0.11	0.11	0.10			
1 Week	Mean	6.48	1.08	36,967[3]	16,326[3]	0.039	0.042
(n = 5)	SEM	0.71	4,806	1,959			
	CV	0.11	0.13	0.12			
4 Weeks	Mean	5.97[2]	1.18	81,148	13,326[3]	0.048	0.047
(n = 5)	SEM	0.48	8,926	1,733			
	CV	0.08	0.11	0.13			

[1]SEM, standard error of the mean; CV, coefficient of variation; V, volume; CF, correction (shrinkage) factor; C, total number of cells; CE (C), coefficient of error of the total number of cells.
[2]$P < 0.05$ vs. control.
[3]$P < 0.01$ vs. control.

RESULTS

Control

CA1 region. TASK-1 immunoreactive (TASK-1^+) astrocytes were abundantly localized in the stratum oriens, stratum radiatum, stratum lucidum, and stratum lacunosum-moleculare of the CA1 region. Almost GFAP-immunoreactive ($GFAP^+$) astrocytes showed TASK-1 immunoreactivity (Fig. 2A–C).

Dentate gyrus. TASK-1 immunoreactivity was strongly detected in astrocytes in the molecular layer and the hilus of the dentate gyrus. Almost $GFAP^+$ astrocytes showed TASK-1 immunoreactivity (Fig. 2A,D,E).

One day after SE

CA1 region. The processes of TASK-1^+ astrocytes became unevenly thick, with ragged edges in the CA1 region. These TASK-1^+ astrocytes showed strong GFAP immunoreactivity (Fig. 3A–C). There was no difference in the total number of TASK-1^+ astrocytes, the volume of the CA1 region, and the ratio of $TASK^+$ astrocytes in GFAP immunoreactive ($GFAP^+$) astrocytes from control (Table 1, see Fig. 4A).

Dentate gyrus. Similar to control animals, GFAP immunoreactivity was strongly detected in astrocytes in the molecular layer and the hilus of the dentate gyrus (Fig. 3A,D,E). The total number of $GFAP^+$ astrocytes in the dentate gyrus was similar to that of control animals (Table 2). Because TASK-1 immunoreactivity in $GFAP^+$ astrocytes was markedly reduced (Figs. 3A,D,E, 4B), the total numbers of TASK-1^+ astrocyte were significantly reduced compared with control animals ($P < 0.05$, Table 2). However, there was no difference in the volume of the molecular layer from control (Table 2).

One week after SE

CA1 region. One week after SE (latent or epileptogenic period; Fig. 5), TASK-1^+ astrocytes in the CA1 region showed hypertrophy of the cell bodies and processes of astrocytes. These hypertrophic TASK-1^+ astrocytes showed strong $GFAP^+$ immunoreactivity (Fig. 5A–C). There was no difference in the total number of TASK-1^+ astrocytes, the volume of the CA1 region, or the ratio of $TASK^+$ astrocytes in $GFAP^+$ astrocytes from control (Table 1, Fig. 4A).

Dentate gyrus. Consistently with our previous study (Kang et al., 2006), loss of $GFAP^+$ astrocytes was observed in the molecular layer of the dentate gyrus at 1 week after SE ($P < 0.01$ vs. control; Fig. 4B, Table 2). The disappearance of $GFAP^+$ astrocytes was pronounced from the inner molecular layer to the outer molecular layer, indicating that the network of astrocytes had been disrupted (Fig. 5A,D,E). Because of astroglial loss, TASK-1^+ immunoreactivity was also reduced in the molecular layer of the dentate gyrus (Figs. 4B, 5A,D,E). Therefore, the total number of TASK-1^+ astrocytes was significantly reduced in the molecular layer of the dentate gyrus ($P < 0.01$ vs. control; Table 2). There was no difference in the volume of the molecular layer from control (Table 2). In contrast to

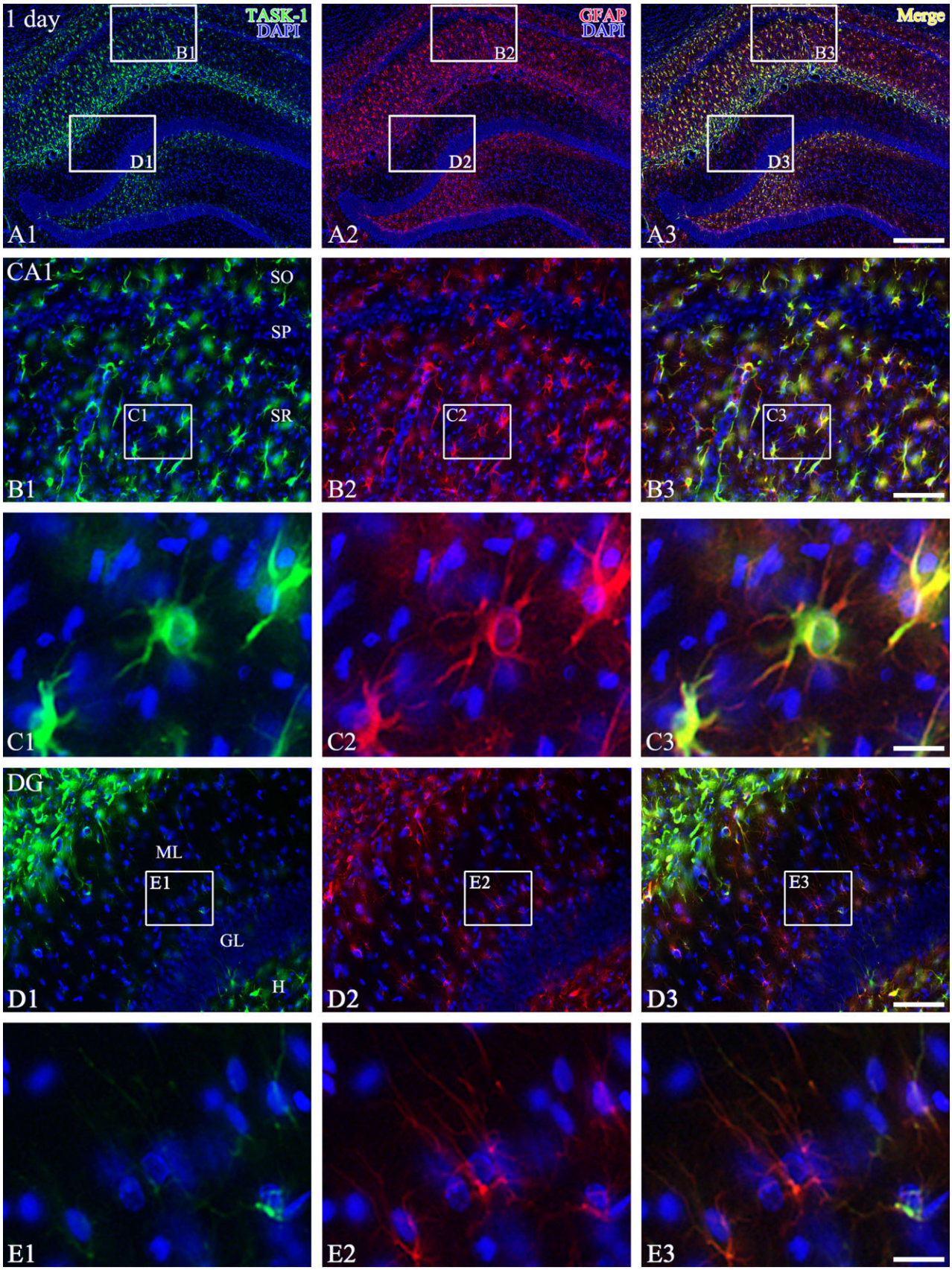

Fig. 3. **A–E:** TASK-1 (green) and GFAP (red) signals in the hippocampal complex at 1 day after SE. In the CA1 region (B,C), TASK-1 immunoreactivity is unaltered in GFAP$^+$ astrocytes compared with controls. In the dentate gyrus (D,E), however, TASK-1 immunoreactivity in GFAP$^+$ astrocytes is markedly decreased. Panels 1, 2, and 3 are TASK-1, GFAP, and merged images, respectively. Blue is DAPI counterstaining. GL, granule cell layer; H, hilus; ML, molecular layer; SO, stratum oriens; SP, stratum pyramidale; SR, stratum radiatum. Scale bars = 200 μm in A; 50 μm in B,D; 10 μm in C,E.

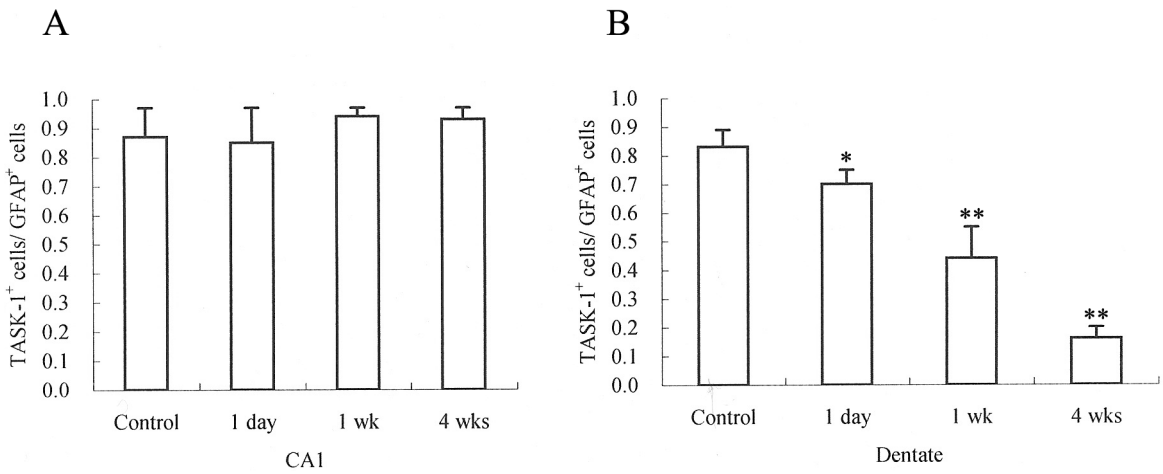

Fig. 4. Comparison of the colocalization of TASK-1 immunoreactivity in GFAP$^+$ astrocytes following SE. **A:** The ratio of TASK-1$^+$ immunoreactivity in GFAP$^+$ astrocytes in the CA1 region following SE (mean ± SEM). **B:** The ratio of TASK-1$^+$ immunoreactivity in GFAP$^+$ astrocytes in the dentate gyrus following SE (mean ± SEM). Unlike the CA1 region, TASK-1 immunoreactivity is reduced in GFAP$^+$ astrocytes in the dentate gyrus following SE. Significant differences from the controls, $^*P < 0.05$, $^{**}P < 0.01$.

the molecular layer, TASK-1$^+$ cells were strongly detected in the subgranular region (Fig. 6). These cells had bipolar, elongated cell bodies with fusiform-shaped nuclei, and these bipolar cells showed Vim immunoreactivity. Some Vim$^+$ cells with branched processes were also located in the inner molecular layer of the dentate gyrus. However, these Vim$^+$ cells showed very weak TASK-1 immunoreactivity.

Four weeks after SE

CA1 region. After recurrent seizure onset (4 weeks after SE; Fig. 7A–C), GFAP$^+$ astrocytes showed typical reactive gliosis (hypertrophy and hyperplasia of cell bodies and processes of astrocytes) in the CA1 region. GFAP$^+$ astrocytes in the CA1 region showed strong TASK-1 immunoreactivity. At this time point, animals showed atrophy of the CA1 region (76% of controls). These findings were consistent with previous studies demonstrating reductions in hippocampal volumes following SE (Roch et al., 2002; Niessen et al., 2005). However, there was no difference of the total number of TASK-1$^+$ astrocytes from control (Table 1, Fig. 4A).

Dentate gyrus. GFAP$^+$ astrocytes showed typical reactive gliosis in the dentate gyrus (Fig. 7A,D,E). At this time point, the volume of the molecular layer of the dentate gyrus was 84.9% that of controls. However, the total number of GFAP$^+$ astrocytes in the dentate gyrus recovered to the control level (Fig. 4B, Table 2). Approximately 16% of GFAP$^+$ astrocytes in the molecular layer of the dentate gyrus showed TASK-1 immunoreactivity ($P < 0.01$; Figs. 4B, 7D,E, Table 2).

DISCUSSION

Region-specific distribution of TASK-1 in the hippocampal complex following SE

In the present study, TASK-1 immunoreactivity was abundantly observed in astrocytes within the normal hippocampal complex. These findings are consistent with previous studies demonstrating the localization of TASK-1 in the rat hippocampal complex (Kindler et al., 2000; Talley et al., 2000). After SE, the total numbers of TASK-1$^+$ astrocytes and GFAP$^+$ astrocytes were unaltered in the CA1 region, although the volume of CA1 region was reduced at 4 weeks after SE. These findings indicate that SE may not affect astrocytes in the CA1 region.

In contrast to the CA1 region, the total number of TASK-1$^+$ astrocytes in the molecular layer of the dentate gyrus was significantly reduced in the latent period (1 day to 1 week after SE), although the volume was unaltered. Based on our previous study (Kang et al., 2006), reduced TASK-1 immunoreactivity in the molecular layer may be due to astroglial degeneration. Furthermore, TASK-1$^+$/Vim$^+$ astrocytes (bipolar elongated cells) were detected mainly in the subgranular region. However, some Vim$^+$ cells located in the inner molecular layer showed no TASK-1 immunoreactivity. These findings indicate that TASK-1 immunoreactivity was transiently increased in immature astroglia. Immature Vim$^+$ astrocytes appear to be bipolar elongated cells, and the morphological organization and phenotype of these cells are modified during the course of their maturation, which is accompanied by a progressive increase in GFAP expression (Lendahl et al., 1990; Sancho-Tello et al., 1995). Our previous study (Kang et al., 2006) demonstrated that proliferative astroglia in the subgranular zone migrate into the molecular layer of the dentate gyrus. Furthermore, Bordey and Sontheimer (1997) reported that immature astrocytes showed a strong outwardly rectifying K$^+$ current, which was gradually decreased during postnatal development. Furthermore, the outwardly rectifying K$^+$ current is important in growth control and cell proliferation in astroglia (Sontheimer, 1994). With respect to these previous studies, our findings indicate that transient TASK-1 expression in Vim$^+$ astrocytes may be involved in the enhancement of outwardly rectifying K$^+$ current in newly generated astrocytes, which plays a role in the proliferation or migration after astroglial loss.

Four weeks after SE (when spontaneous seizure developed), in the present study, the total number of GFAP$^+$

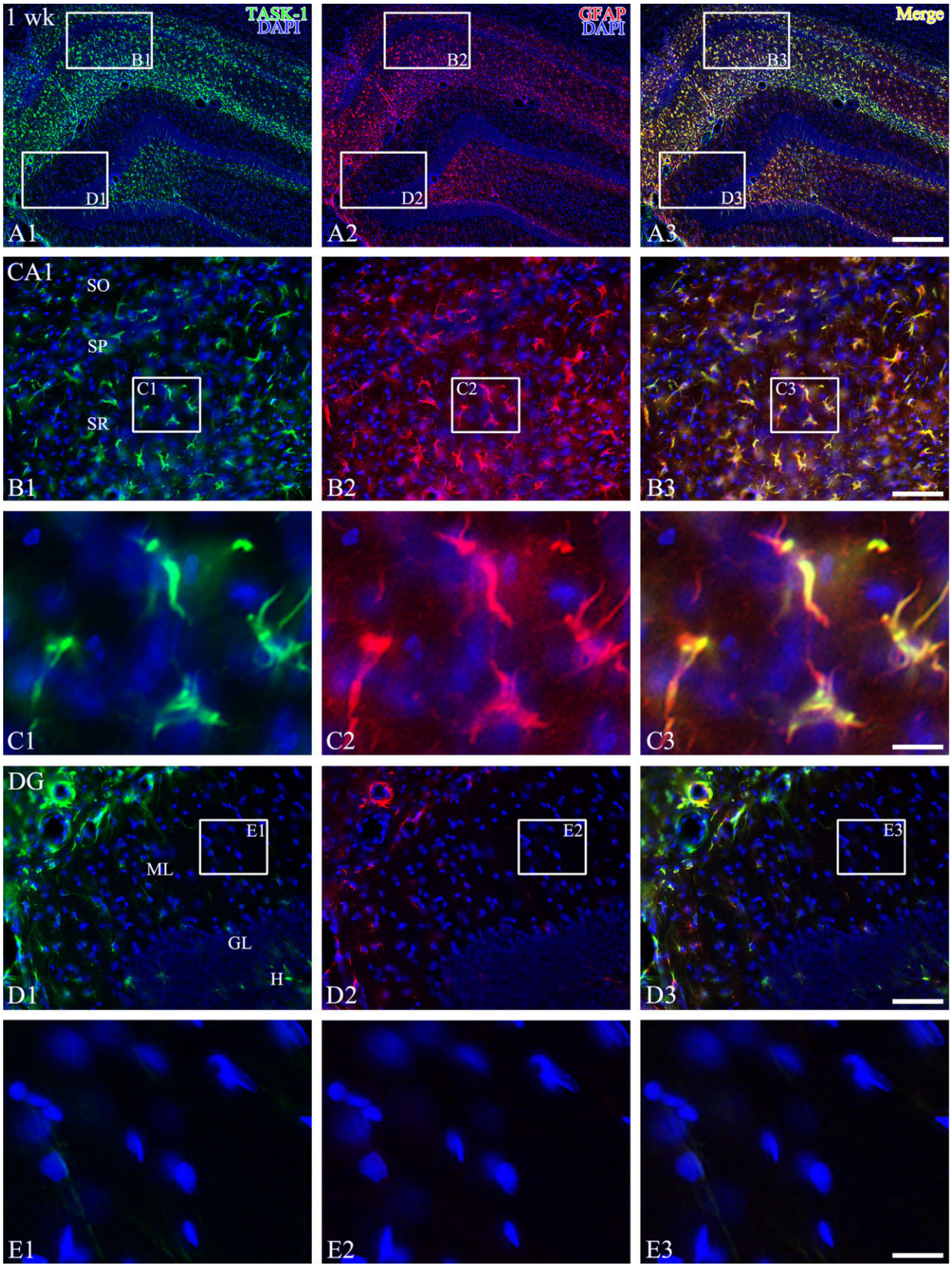

Fig. 5. **A–E:** TASK-1 (green) and GFAP (red) signals in the hippocampal complex at 1 week after SE. In the CA1 region (B,C), hypertrophic astrocytes show strong GFAP and TASK-1 immunoreactivity. In dentate gyrus (D,E), both GFAP and TASK-1 immunoreactivity is rarely detected in the molecular layer. Panels 1, 2, and 3 are TASK-1, GFAP, and merged images, respectively. Blue is DAPI counterstaining. GL, granule cell layer; H, hilus; ML, molecular layer; SO, stratum oriens; SP, stratum pyramidale; SR, stratum radiatum. Scale bars = 200 μm in A; 50 μm in B,D; 10 μm in C,E.

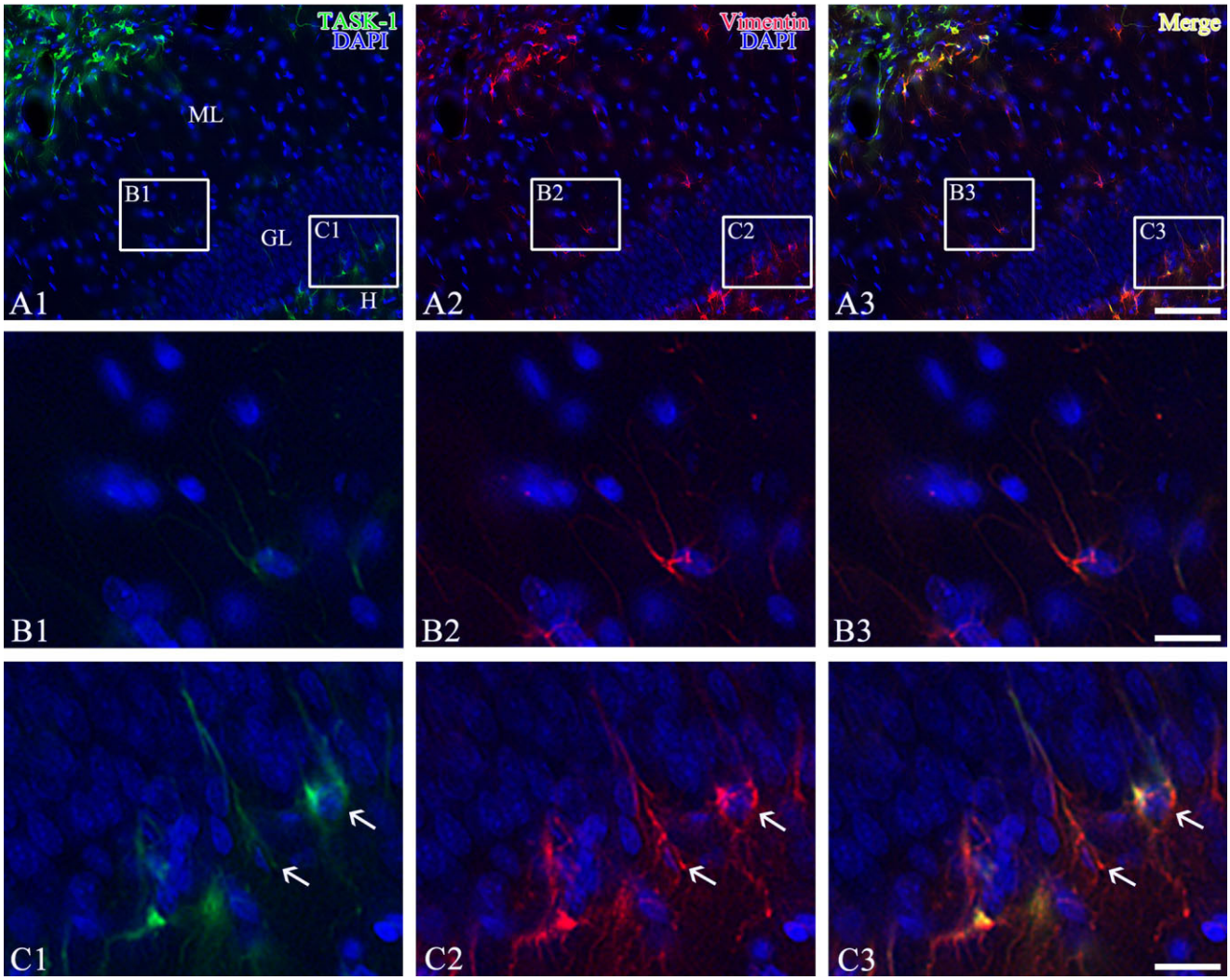

Fig. 6. **A–C:** Double immunofluorescence for TASK-1 (green) and vimentin (red) in the dentate gyrus at 1 week after SE. Vimentin-positive astrocytes in subgranular region contain TASK-1 immunoreactivity (arrows). Blue is DAPI counterstaining. Panels 1, 2, and 3 are TASK-1, vimentin and merge images, respectively. GL, granule cell layer; H, hilus; ML, molecular layer. Scale bars = 50 μm in A; 10 μm in B,C.

astrocytes had recovered to control level, although the volume of molecular layer of the dentate gyrus was reduced to 85% of control level. However, only 16% of reactive astrocytes in the molecular layer of the dentate gyrus showed TASK-1 immunoreactivity. These findings indicate that the loss of TASK-1 immunoreactivity might not be related to alterations in hippocampal atrophy or prolonged astroglial loss. In comparison with those of naïve astrocytes, the functional properties (i.e., responsiveness to glutamate, characteristics of Ca^{2+} oscillations and K^+ buffering) of reactive astrocytes are quite distinct (Kimelberg et al., 1982; Kraig et al., 1986; Lee et al., 1995; Lascola and Kraig, 1997; Gabriel et al., 1998; Matsushima et al., 1998; Kang et al., 2006). Indeed, the loss or down-regulation of GS is particularly pronounced in regions of severe neuronal loss and astroglial proliferation within the hippocampi of epilepsy patients (Eid et al., 2004; van del Hel et al., 2005). Therefore, down-regulations of TASK-1 immunoreactivity in astrocytes within the dentate gyrus at 4 weeks after SE may be a consequence of gliogenesis rather than the transient dedifferentiations of naïve astrocytes. Alternatively, persistent extracellular acidosis induced by repeated spontaneous seizure might also be involved in reduction in astroglial TASK-1 expression in the dentate gyrus (see below).

Functional implication in the distinct astroglial TASK-1 expression in the hippocampal complex

It is well established that the epileptic hippocampal complex shows differential properties between the dentate gyrus and the CA1 region in various experimental models. In the dentate gyrus, paired pulse inhibition is enhanced (Doherty and Dingledine, 2001; Kobayashi and Buckmaster, 2003; Cohen et al., 2003; Leroy et al., 2004; Kwak et

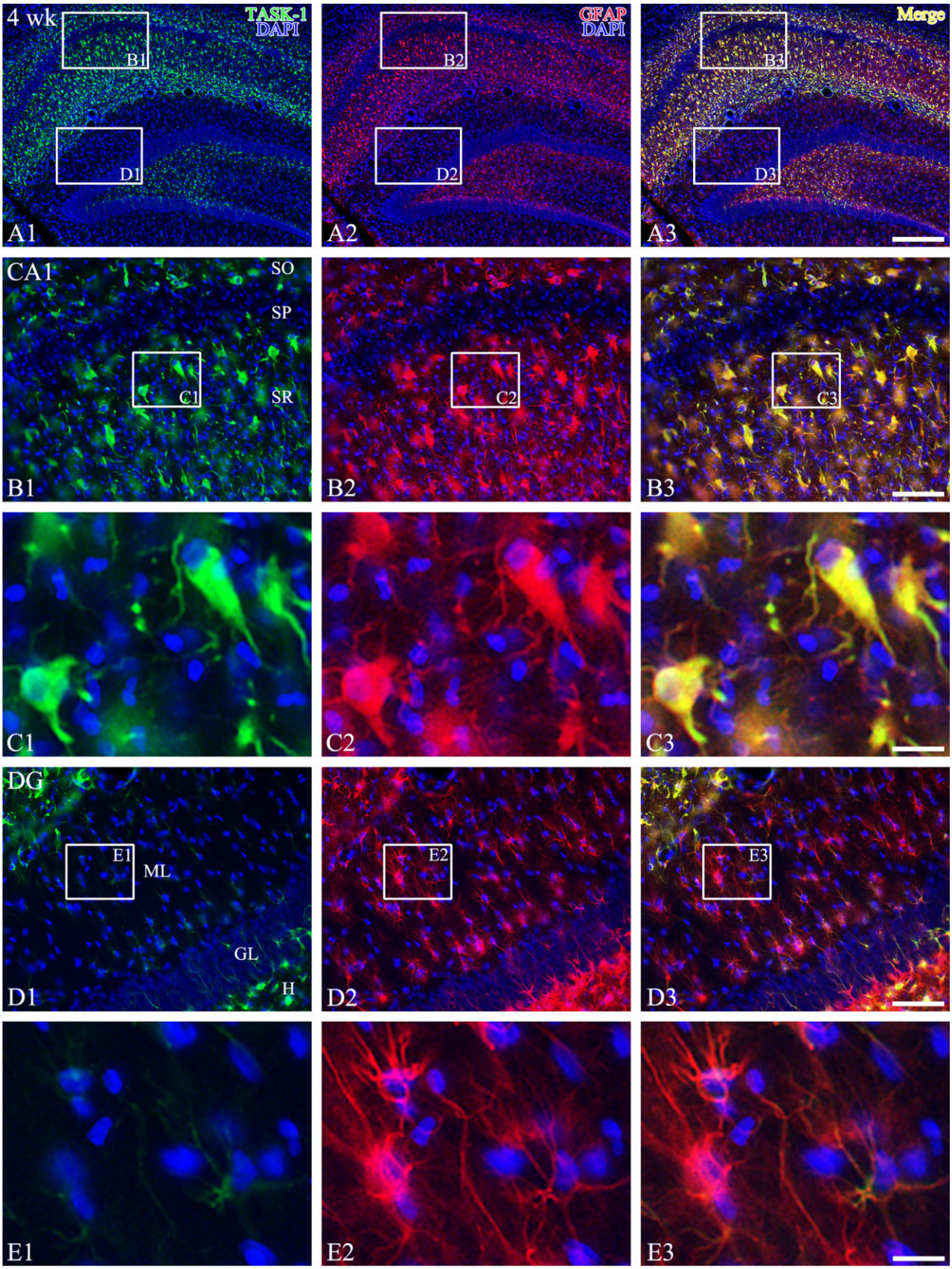

Fig. 7. **A–E:** Double immunofluorescent image of TASK-1 (green) and GFAP (red) at 4 week after SE. In the CA1 region (B,C), reactive astrocytes contain strong TASK-1 immunoreactivity. In the dentate gyrus (D,E), TASK-1$^+$ astrocytes are rarely detected, although GFAP immunoreactivity is strongly observed in reactive astrocytes in the molecular layer. Panels 1, 2, and 3 are TASK-1, GFAP, and merged images, respectively. Blue is DAPI counterstaining. GL, granule cell layer; H, hilus; ML, molecular layer; SO, stratum oriens; SP, stratum pyramidale; SR, stratum radiatum. Scale bars = 200 μm in A; 50 μm in B,D; 10 μm in C,E.

al., 2006), but, in the CA1 region, it is markedly reduced (Wu and Leung, 2003; Wozny et al., 2005; Kwak et al., 2006). In addition, Xiong and Stringer (2000) have reported that, in the CA1 region, recurrent epileptiform activity results in biphasic pH shifts, consisting of an initial extracellular alkalinization, followed by a slower acidification. In contrast, in the dentate gyrus, seizure activity induces only extracellular acidification. Furthermore, Xiong and Stringer suggested that the early extracellular alkalosis might increase excitability in the CA1 region because of reductions in $GABA_A$ receptor inhibition and enhancement in N-methyl-D-aspartate (NMDA) receptor currents, and the later extracellular acidosis might be involved in seizure termination.

Four weeks after SE, in the present study, reactive astrocytes in the molecular layer of the dentate gyrus showed no TASK-1 immunoreactivity, whereas TASK-1^+ reactive astrocytes were abundant in the CA1 region. In agreement with the present data, we have recently reported that, in the hippocampal complex of seizure-prone gerbils (a genetic epilepsy model), TASK-1 immunoreactivity in CA1 astrocytes was higher than that in astrocytes within the dentate gyrus (Kim et al., 2007). Insofar as TASK currents are highly sensitive to extracellular pH [low extracellular pH (below 6.5) inhibits TASK currents, whereas high extracellular pH (about 8.7) potentiates them] (for review see Brown, 2000), it is conceivable that the different expression patterns of TASK-1 between CA1 and dentate gyrus might be involved in the differential physiological properties and generation of seizure activity between CA1 and dentate gyrus: After recurrent epileptiform activity, in the CA1 region, activation of TASK-1 channels by the initial extracellular alkalosis would increase astroglial outwardly K^+ rectification. In this situation, extracellular K^+ concentration would be elevated, which prolongs neuronal depolarization. In contrast to the CA1 region, down-regulation of astroglial TASK-1 channels (by either persistent extracellular acidification or changed properties of newly generated astrocytes) in the dentate gyrus could effectively contribute to rapid neuronal repolarization by maintenance of low extracellular K^+ level. Therefore, our findings indicate that the different expression patterns of astroglial TASK-1 expression may be involved in the differential physiological properties and seizure susceptibilities between CA1 and dentate gyrus in the hippocampal complex.

In conclusion, our findings indicate that TASK-1 immunoreactivity was differentially altered in astrocytes located in different regions of the hippocampal complex following SE, and this change was affected by astroglial degeneration/regeneration. Therefore, alteration in TASK-1 immunoreactivity may contribute to acquisition of the properties of the epileptic hippocampal complex.

LITERATURE CITED

Bacci A, Verderio C, Pravettoni E, Matteoli M. 1999. The role of glial cells in synaptic function. Philos Trans R Soc Lond B Biol Sci 354:403–409.

Bedi KS. 1991. Effects of undernutrition during early life on granule cell numbers in the rat dentate gyrus. J Comp Neurol 311:425–433.

Bordey A, Sontheimer H. 1997. Postnatal development of ionic currents in rat hippocampal astrocytes in situ. J Neurophysiol 78:461–477.

Brown DA. 2000. Neurobiology: the acid test for resting potassium channels. Curr Biol 10:R456–R459.

Cohen AS, Lin DD, Quirk GL, Coulter DA. 2003. Dentate granule cell $GABA_A$ receptors in epileptic hippocampus: enhanced synaptic efficacy and altered pharmacology. Eur J Neurosci 17:1607–1616.

DeLorenzo RJ, Pellock JM, Towne AR, Boggs JG. 1995. Epidemiology of status epilepticus. J Clin Neurophysiol 12:316–325.

Doherty J, Dingledine R. 2001. Reduced excitatory drive onto interneurons in the dentate gyrus after status epilepticus. J Neurosci 21:2048–2057.

Duprat F, Lesage F, Fink M, Reyes R, Heurteaux C, Lazdunski M. 1997. TASK, a human background K^+ channel to sense external pH variations near physiological pH. EMBO J 16:5464–5471.

Eid T, Thomas MJ, Spencer DD, Runden-Pran E, Lai JC, Malthankar GV, Kim JH, Danbolt NC, Ottersen OP, de Lanerolle NC. 2004. Loss of glutamine synthetase in the human epileptogenic hippocampus: possible mechanism for raised extracellular glutamate in mesial temporal lobe epilepsy. Lancet 363:28–37.

Fields RD, Stevens-Graham B. 2002. New insights into neuron–glia communication. Science 298:556–562.

Fujikawa DG. 1995. Neuroprotective effect of ketamine administered after status epilepticus onset. Epilepsia 36:186–195.

Gabriel S, Kivi A, Eilers A, Kovács R, Heinemann U. 1998. Effects of barium on stimulus-induced rises in $[K^+]o$ in juvenile rat hippocampal area CA1. Neuroreport 9:2583–2587.

Kang TC, Kim DS, Kwak SE, Kim JE, Won MH, Kim DW, Choi SY, Kwon OS. 2006. Epileptogenic roles of astroglial death and regeneration in the dentate gyrus of experimental temporal lobe epilepsy. Glia 54:258–271.

Kim DS, Kim JE, Kwak SE, Choi HC, Song HK, Kimg YI, Choi SY, Kang TC. 2007. Up-regulated astroglial TWIK-related acid-sensitive K^+ channel-1 (TASK-1) in the hippocampus of seizure-sensitive gerbils: a target of anti-epileptic drugs. Brain Res 1185:346–358.

Kim Y, Bang H, Kim D. 2000. TASK-3, a novel tandem pore domain acid-sensitive K^+ channel. An extracellular histidin as pH sensor. J Biol Chem 275:9340–9347.

Kimelberg HK, Stieg PE, Mazurkiewicz ZE. 1982. Immunocytochemical and biochemical analysis of carbonic anhydrase in primary astrocyte cultures from rat brain. J Neurochem 39:734–742.

Kindler CH, Pietruck C, Yost CS, Sampson ER, Gray AT. 2000. Localization of the tandem pore domain K^+ channel TASK-1 in the rat central nervous system. Brain Res Mol Brain Res 98:99–108.

Kobayashi M, Buckmaster PS. 2003. Reduced inhibition of dentate granule cells in a model of temporal lobe epilepsy. J Neurosci 23:2440–2452.

Kraig RP, Pulsinelli WA, Plum F. 1986. Carbonic acid buffer changes during complete brain ischemia. Am J Physiol 250:R348–R357.

Kwak SE, Kim JE, Kim DS, Won MH, Lee HJ, Choi SY, Kwon OS, Kim JS, Kang TC. 2006. Differential paired-pulse responses between the CA1 region and the dentate gyrus are related to altered CLC-2 immunoreactivity in the pilocarpine-induced rat epilepsy model. Brain Res 1115:162–168.

Lascola C, Kraig RP. 1997. Astroglial acid-base dynamics in hyperglycemic and normoglycemic global ischemia. Neurosci Biobehav Rev 21:143–150.

Lee SH, Magge S, Spencer DD, Sontheimer H, Cornell-Bell AH. 1995. Human epileptic astrocytes exhibit increased gap junction coupling. Glia 15:195–202.

Lendahl U, Zimmerman LB, McKay RD. 1990. CNS stem cells express a new class of intermediate filament protein. Cell 60:585–595.

Leonoudakis D, Gray AT, Winegar BD, Kindler CH, Harada M, Taylor DM, Chavez RA, Forsayeth JR, Yost CS. 1998. An open rectifier potassium channels with two pore domains in tandem cloned from rat cerebellum. J Neurosci 18:868–877.

Leroy C, Poisbeau P, Keller AF, Nehlig A. 2004. Pharmacological plasticity of $GABA_A$ receptors at dentate gyrus synapses in a rat model of temporal lobe epilepsy. J Physiol 557:473–487.

Madeira MD, Sousa N, Santer RM, Paula-Barbosa MM, Gundersen HJ. 1995. Age and sex do not affect the volume, cell numbers, or cell size of the suprachiasmatic nucleus of the rat: an unbiased stereological study. J Comp Neurol 361:585–601.

Matsushima K, Schmidt-Kastner R, Hogan MJ, Hakim AM. 1998. Cortical spreading depression activates trophic factor expression in neurons and astrocytes and protects against subsequent focal brain ischemia. Brain Res 5:47–60.

Millar JA, Barratt L, Southan AP, Page KM, Fyffe RE, Robertson B, Mathie A. 2000. A functional role for the two-pore domain potassium channel TASK-1 in cerebellar granule neurons. Proc Natl Acad Sci U S A 97:3614–3618.

Niemeyer MI, Gonzalez-Nilo FD, Zuniga L, Gonzalez W, Cid LP, Sepulveda

FV. 2006. Gating of two-pore domain K^+ channels by extracellular pH. Biochem Soc Trans 34:899–902.

Niessen HG, Angenstein F, Vielhaber S, Frisch C, Kudin A, Elger CE, Heinze HJ, Scheich H, Kunz WS. 2005. Volumetric magnetic resonance imaging of functionally relevant structural alterations in chronic epilepsy after pilocarpine-induced status epilepticus in rats. Epilepsia 46:1021–1026.

Pecchi E, Dallaporta M, Charrier C, Pio J, Jean A, Moyse E, Troadec JD. 2007. Glial fibrillary acidic protein (GFAP)-positive radial-like cells are present in the vicinity of proliferative progenitors in the nucleus tractus solitarius of adult rat. J Comp Neurol 501:353–368.

Racine RJ. 1972. Modification of seizure activity by electrical stimulation. II. Motor seizure. Electroencephalogr Clin Neurophysiol 32:281–294.

Rau KK, Cooper BY, Johnson RD. 2006. Expression of TWIK-related acid sensitive K^+ channels in capsaicin sensitive and insensitive cells of rat dorsal root ganglia. Neuroscience 141:955–963.

Reyes R, Duprat F, Lesage F, Fink M, Salinas M, Farman N, Lazdunski M. 1998. Cloning and expression of a novel pH-sensitive two pore domain K^+ channel from human kidney. J Biol Chem 273:30863–30869.

Rice AC, DeLorenzo RJ. 1998. NMDA receptor activation during status epilepticus is required for the development of epilepsy. Brain Res 782:240–247.

Roch C, Leroy C, Nehlig A, Namer IJ. 2002. Magnetic resonance imaging in the study of the lithium-pilocarpine model of temporal lobe epilepsy in adult rats. Epilepsia 43:325–335.

Rossetti AO, Logroscino G, Liaudet L, Ruffieux C, Ribordy V, Schaller MD, Despland PA, Oddo M. 2007. Status epilepticus: an independent outcome predictor after cerebral anoxia. Neurology 69:255–260.

Sancho-Tello M, Valles S, Montoliu C, Renau-Piqueras J, Guerri C. 1995. Developmental pattern of GFAP and vimentin gene expression in rat brain and in radial glial cultures. Glia 15:157–166.

Shetty AK, Turner DA. 2000. Fetal hippocampal grafts containing CA3 cells restore host hippocampal glutamate decarboxylase-positive interneuron numbers in a rat model of temporal lobe epilepsy. J Neurosci 20:8788–8801.

Sontheimer H. 1994. Voltage-dependent ion channels in glial cells. Glia 11:156–172.

Stewart LS, Persinger MA. 2001. Ketamine prevents learning impairment when administered immediately after status epilepticus onset. Epilepsy Behav 2:585–591.

Talley EM, Lei Q, Sirois JE, Bayliss DA. 2000. TASK-1, a two pore domain K^+ channel, is modulated by multiple neurotransmitters in motoneurons. Neuron 25:399–410.

van der Hel WS, Notenboom RG, Bos IW, van Rijen PC, van Veelen CW, de Graan PN. 2005. Reduced glutamine synthetase in hippocampal areas with neuron loss in temporal lobe epilepsy. Neurology 64:326–333.

Wozny C, Gabriel S, Jandova K, Schulze K, Heinemann U, Behr J. 2005. Entorhinal cortex entrains epileptiform activity in CA1 in pilocarpine-treated rats. Neurobiol Dis 19:451–460.

Wu K, Leung LS. 2003. Increased dendritic excitability in hippocampal ca1 in vivo in the kainic acid model of temporal lobe epilepsy: a study using current source density analysis. Neuroscience 116:599–616.

Xiong ZQ, Stringer JL. 2000. Extracellular pH responses in CA1 and the dentate gyrus during electrical stimulation, seizure discharges, and spreading depression. J Neurophysiol 83:3519–3524.

Yang P, Baker KA, Hagg T. 2005. A disintegrin and metalloprotease 21 (ADAM21) is associated with neurogenesis and axonal growth in developing and adult rodent CNS. J Comp Neurol 490:163–179.